7-17-2012

Modeling potential hydrochemical responses to climate change and increasing CO2 at the Hubbard Brook Experimental Forest using a dynamic biogeochemical model (PnET-BGC)

Afshin Pourmokhtaria
Syracuse University

Charles T. Driscoll
Syracuse University

John L. Campbell
Northern Research Station, U.S Forest Service

Katharine Hayhoe
Texas Tech University

Modeling potential hydrochemical responses to climate change and increasing CO_2 at the Hubbard Brook Experimental Forest using a dynamic biogeochemical model (PnET-BGC)

Afshin Pourmokhtarian,[1] Charles T. Driscoll,[1] John L. Campbell,[2] and Katharine Hayhoe[3]

Received 2 August 2011; revised 1 May 2012; accepted 14 May 2012; published 17 July 2012.

[1] Dynamic hydrochemical models are useful tools for understanding and predicting the interactive effects of climate change, atmospheric CO_2, and atmospheric deposition on the hydrology and water quality of forested watersheds. We used the biogeochemical model, PnET-BGC, to evaluate the effects of potential future changes in temperature, precipitation, solar radiation, and atmospheric CO_2 on pools, concentrations, and fluxes of major elements at the Hubbard Brook Experimental Forest in New Hampshire, United States. Future climate projections used to run PnET-BGC were generated specifically for the Hubbard Brook Experimental Forest with a statistical technique that downscales climate output (e.g., air temperature, precipitation, solar radiation) from atmosphere-ocean general circulation models (AOGCMs) to a finer temporal and spatial resolution. These climate projections indicate that over the twenty-first century, average air temperature will increase at the site by 1.7°C to 6.5°C with simultaneous increases in annual average precipitation ranging from 4 to 32 cm above the long-term mean (1970–2000). PnET-BGC simulations under future climate change show a shift in hydrology characterized by later snowpack development, earlier spring discharge (snowmelt), greater evapotranspiration, and a slight increase in annual water yield (associated with CO_2 effects on vegetation). Model results indicate that under elevated temperature, net soil nitrogen mineralization and nitrification markedly increase, resulting in acidification of soil and stream water, thereby altering the quality of water draining from forested watersheds. Invoking a CO_2 fertilization effect on vegetation under climate change substantially mitigates watershed nitrogen loss, highlighting the need for a more thorough understanding of CO_2 effects on forest vegetation.

Citation: Pourmokhtarian, A., C. T. Driscoll, J. L. Campbell, and K. Hayhoe (2012), Modeling potential hydrochemical responses to climate change and increasing CO_2 at the Hubbard Brook Experimental Forest using a dynamic biogeochemical model (PnET-BGC), *Water Resour. Res.*, *48*, W07514, doi:10.1029/2011WR011228.

1. Introduction

[2] In the northeastern United States, air temperature has been increasing at a rate of nearly 0.27°C per decade since 1970 [*Northeast Climate Impact Assessment (NECIA)*, 2006]. Changes in precipitation are more variable, but regionally show an overall average increase of 100 mm over the same time period [*Hayhoe et al.*, 2007]. Climate projections from coupled atmosphere-ocean general circulation models (AOGCMs) suggest that, across the northeastern U. S., annual average air temperature and precipitation will continue to increase over the twenty-first century. The extent of these increases depends on future green house gas emissions; a lower emissions scenario (B1) is projected to increase air temperature by 2.1°C and annual precipitation 7%, while a higher emissions scenario (A1fi) would increase air temperature by 5.3°C and precipitation by 14%, with larger changes in winter and spring as compared to summer and fall [*Hayhoe et al.*, 2007, 2008].

[3] The direct and indirect effects of climate change on terrestrial and aquatic ecosystems are likely to be complex and highly variable in time and space [*Campbell et al.*, 2009]. Climatic effects should not be studied in isolation from other aspects of global change, such as atmospheric deposition and land disturbance. The combined influence of multiple factors contributes to the complexity of assessing the effects of global climate change on forest ecosystems.

[4] The coarse spatial resolution (~100 km) of AOGCM output has been particularly problematic for use as climate input to hydrochemical models that are run at the local scale. This issue is particularly challenging in small, high-elevation watersheds in complex mountainous terrain because these areas are strongly affected by local weather patterns. High-elevation watersheds nevertheless, are critically important

[1]Department of Civil and Environmental Engineering, Syracuse University, Syracuse, New York, USA.
[2]Northern Research Station, U.S. Forest Service, Durham, New Hampshire, USA.
[3]Department of Political Science, Texas Tech University, Lubbock, Texas, USA.

Corresponding author: A. Pourmokhtarian, Department of Civil and Environmental Engineering, 151 Link Hall, Syracuse University, Syracuse, NY 13244, USA. (apourmok@syr.edu)

0043-1397/12/2011WR011228

for managing water supplies. Recently, statistical techniques have been developed to downscale coarse resolution AOGCM output to a finer spatial resolution [*Hayhoe et al.*, 2004, 2007, 2008]. In this study we used these statistically downscaled projections of temperature, precipitation, and photosynthetically active radiation (PAR) as model input, enabling simulations of future hydrochemistry at the small watershed scale. Understanding the use of AOGCM output in the application of hydrochemical models should improve quantification of the direct and indirect effects of climate change on water resources.

[5] The objective of this study was to use the hydrochemical model, PnET-BGC, to evaluate the direct and indirect effects of global change drivers (i.e., temperature, precipitation, solar radiation, CO_2) on biogeochemical processes in a northern hardwood forest ecosystem at the Hubbard Brook Experimental Forest (HBEF) in New Hampshire. A sensitivity analysis was conducted to better understand how the model responds to variations in climatic drivers, including air temperature, precipitation, and PAR. This analysis improves the understanding of the potential consequences of changing climate in high-elevation forest watersheds, and the strengths and limitations of using AOGCM-derived climate projections as input to hydrochemical watershed models.

2. Methods

2.1. Site Description

[6] The HBEF is located in the southern White Mountains of New Hampshire (43°56′N, 71°45′W) [*Likens and Bormann*, 1995]. The site was established by the U. S. Forest Service in 1955 as a center for hydrological research, and in 1987 it was designated as a National Science Foundation Long-Term Ecological Research (LTER) site. The climate is humid continental, with short, cool summers and long, cold winters. Soils are well-drained Spodosols with an average depth of 1–2 m. Vegetation is mostly northern hardwood, dominated by sugar maple (*Acer saccharum*), American beech (*Fagus grandifolia*), and yellow birch (*Betula alleghaniensis*). Conifer species are more prevalent at higher elevations, consisting largely of balsam fir (*Abies balsamea*) and red spruce (*Picea rubens*) [*Johnson et al.*, 2000].

[7] The model was run for watershed 6 (W6), which has one of the longest continuous records of meteorology, hydrology, and biogeochemistry in the U. S. [*Likens and Bormann*, 1995; *Likens et al.*, 1994] (available at http://www.hubbardbrook.org/). The watershed area is 13.2 ha, with an elevation range of 549–792 m. Watershed 6 was logged intensively from 1910 to 1917, and has experienced some subsequent disturbances including a hurricane in 1938, which prompted some salvage logging, and an ice storm in 1998.

2.2. PnET-BGC

[8] PnET-BGC is a biogeochemical model that has been used to evaluate the effects of climate change, atmospheric deposition, and land disturbance on soil and surface waters in northern forest ecosystems [*Chen and Driscoll*, 2005]. PnET-BGC was created by linking the forest-soil-water model PnET-CN [*Aber and Driscoll*, 1997; *Aber et al.*, 1997] with a biogeochemical (BGC) submodel [*Gbondo-Tugbawa et al.*, 2001], thereby enabling the simultaneous simulation of major element cycles (Ca^{2+}, Mg^{2+}, K^+, Na^+, C, N, P, S, Si, Al^{3+}, Cl^-, and F^-). PnET-BGC has been used extensively to evaluate fluxes of water and elements in forest ecosystems by depicting ecosystem processes, including atmospheric deposition, CO_2 effects on vegetation, canopy interactions, plant uptake, litterfall, soil organic matter dynamics, nitrification, mineral weathering, chemical reactions involving gas, solid, and solution phases, and surface water processes [*Gbondo-Tugbawa et al.*, 2001]. These processes determine the hydrochemical characteristics of the ecosystem because water and solutes interact with forest vegetation and soil before emerging as surface runoff.

[9] Model inputs include climatic data (PAR, precipitation, maximum and minimum temperature), atmospheric CO_2 concentration and atmospheric deposition (wet and dry), vegetation type (northern hardwoods, spruce-fir), element stoichiometry, soil characteristics (soil mass, soil cation exchange capacity, element weathering rates, soil cation exchange and anion adsorption coefficients, water holding capacity), and historical land disturbance (e.g., forest harvesting, hurricane, ice storm, fire) [*Chen and Driscoll*, 2005; *Gbondo-Tugbawa et al.*, 2001; *Zhai et al.*, 2008]. A detailed description of PnET-BGC is provided by *Aber and Driscoll*, [1997], *Aber et al.* [1997], and *Gbondo-Tugbawa et al.* [2001], including a sensitivity analysis of parameters.

[10] In this application, the model was run on a monthly time step from year 1000 to 2100. This time frame includes a spin-up period (1000–1850), which allows the model to reach steady state under "background" conditions of climate and atmospheric deposition. Hindcast simulations from 1850 to 2009 were based on estimates of historical climate, atmospheric deposition, and land disturbance. Early values for these inputs were recreated from historical records [*Aber and Federer*, 1992; *Driscoll et al.*, 2001] by matching them with measured values later in the record (for the HBEF meteorology and hydrology since 1955, bulk deposition since 1963, and wet deposition since 1978). The model was run from 2009 through 2100 using future global change scenarios that are based on projected changes in climate, atmospheric CO_2, and business as usual scenarios for atmospheric deposition.

2.3. Algorithm for CO_2 Effects on Vegetation

[11] Although there have been numerous CO_2 enrichment experiments [e.g., *Ainsworth and Long*, 2005; *Ainsworth and Rogers*, 2007; *Ainsworth et al.*, 2002; *Norby et al.*, 1999, 2010], few have occurred in forests [*Ainsworth and Long*, 2005; *Curtis and Wang*, 1998; *Curtis et al.*, 1995; *Ellsworth*, 1999; *Ellsworth et al.*, 1995; *Lewis et al.*, 1996; *Saxe et al.*, 1998], and those have been short duration experiments that have utilized relatively young stands [*Drake et al.*, 1997; *Ellsworth*, 1999; *Nowak et al.*, 2004; *Ollinger et al.*, 2009; *Saxe et al.*, 1998]. Nevertheless, we depicted the effects of increasing atmospheric CO_2 on forests using a multilayered submodel of photosynthesis and phenology developed by *Aber et al.* [1995, 1996], and modified by *Ollinger et al.* [1997, 2002]. There are two confounding effects of atmospheric CO_2 on vegetation: changes in stomatal conductance and a CO_2 fertilization effect on biomass. In order to simulate these effects, stomatal conductance and photosynthesis are coupled [*Jarvis and Davies*, 1998] such that stomatal conductance varies in proportion to changes in ambient CO_2 (C_a) across the boundary of stomata [*Ollinger et al.*, 2002, 2009; *Saxe et al.*, 1998]. Water use efficiency

(WUE) is a function of CO_2 assimilation and is inversely correlated to vapor pressure deficit (VPD) [*Ollinger et al.*, 2002, 2009]. The internal concentration of CO_2 (C_i) is estimated from C_i/C_a which is relatively constant in response to changes in ambient CO_2 [*Beerling*, 1996; *Drake et al.*, 1997; *Ellsworth*, 1999; *Lewis et al.*, 1996; *Nowak et al.*, 2004; *Ollinger et al.*, 2009; *Saxe et al.*, 1998] and varies with changes in foliar N [*Farquhar and Wong*, 1984]. Therefore, the model depicts higher assimilation of CO_2 along with higher depletion of C_i in foliage with higher N [*Ollinger et al.*, 2002, 2009]. A detailed description of the processes and parameters related to photosynthesis in the model are described by *Ollinger et al.* [2009].

2.4. Future Climate Scenarios

[12] In this study we used data from three AOGCMs: the U. S. National Oceanographic and Atmospheric Administration/Geophysical Fluid Dynamics Laboratory model CM2.1 (GFDL) [*Delworth et al.*, 2006], the United Kingdom Meteorological Office Hadley Centre Coupled Model, version 3 (HadCM3) [*Pope et al.*, 2000], and the U. S. Department of Energy/National Center for Atmospheric Research Parallel Climate Model (PCM) [*Washington et al.*, 2000]. These three models have different climate sensitivities in terms of equilibrium of global mean surface air temperature change resulting from a doubling of atmospheric CO_2 concentrations relative to preindustrial conditions (1850). GFDL and HadCM3 have medium to medium-high climate sensitivities (1.5°C–3.4°C and 2.0°C–3.3°C, respectively), while PCM has a low climate sensitivity (1.3°C–2.1°C) [*Hayhoe et al.*, 2007, 2008; *NECIA*, 2006], covering the lower part of the IPCC 1.5°C–4.5°C range [*Intergovernmental Panel on Climate Change (IPCC)*, 2007, *NECIA*, 2006]. We used the Special Report on Emissions Scenarios [*Nakićenović et al.*, 2000] A1fi (fossil fuel-intensive) and B1 scenarios to represent possible higher- and lower-emission futures, respectively. At the end of the current century (2099), atmospheric CO_2 concentrations are estimated to reach 970 (ppm) under the higher emissions scenario (A1fi) and 550 ppm under the lower emissions scenario (B1), which are triple and double preindustrial concentrations, respectively. In total, six climate change scenarios were developed for this application (three AOGCMs times two emissions scenarios).

[13] Monthly, coarse resolution AOGCM temperature, precipitation, and solar radiation output was statistically downscaled to 1/8° resolution for the period of 1960 to 2100 using a standard downscaling routine [*Hayhoe et al.*, 2007, 2008; *Liang et al.*, 1994; *NECIA*, 2006]. A detailed description, comparison, and validation of the AOGCM downscaling method is provided by *Campbell et al.* [2011], *Hayhoe et al.* [2004, 2007, 2008], and *NECIA* [2006] (see auxiliary material).[1]

2.5. Model Application and Validation

[14] To evaluate model performance, we used two statistical indicators: normalized mean error (NME) and normalized mean absolute error (NMAE) [*Janssen and Heuberger*, 1995],

$$\mathrm{NME} = \frac{\overline{P} - \overline{O}}{\overline{O}}, \tag{1}$$

$$\mathrm{NMAE} = \frac{\sum_{i=1}^{n}(|P_i - O_i|)}{n\overline{O}}, \tag{2}$$

where P_i is the predicted value and O_i is the observed value at time i. $\overline{P}$ and $\overline{O}$ are means of the individual observations of P_i and O_i, respectively, and n is the number of observations. NME provides a comparison of the means of predicted and observed values and is an index of relative bias, indicating overestimation (NME $>$ 0) or underestimation (NME $<$ 0) of simulations. The NMAE, which is scaled relative to mean observations, indicates any discrepancy between model simulations and observed values. The smaller the absolute value, the closer model simulations are to observed values.

2.6. Sensitivity Analysis

[15] Building on previous sensitivity analyses for PnET-BGC [*Aber et al.*, 1997; *Gbondo-Tugbawa et al.*, 2001; *Schecher and Driscoll*, 1995], we evaluated the sensitivity of model calculations to climatic inputs: temperature, precipitation, and PAR. The state variables used to assess model sensitivity to these inputs were discharge, stream NO_3^-, DOC, acid neutralizing capacity (ANC), and soil base saturation (BS%). These state variables were selected because of their role in the acid-base status of soil and water and the importance in water supply response to climate change. The sensitivity analysis was conducted by testing the relative change in each state variable X values divided by the relative change in the value of the input (Input) tested [*Gbondo-Tugbawa et al.*, 2001]. Thus, the sensitivity of an input $S_{\mathrm{Input},X}$ is as follows [*Jørgensen*, 1988]:

$$S_{\mathrm{Input},X} = \frac{\partial X/X}{\partial \mathrm{Input}/\mathrm{Input}}. \tag{3}$$

[16] Higher $S_{\mathrm{Input},X}$ values indicate that the model is more sensitive to that climate driver [*Jørgensen*, 1988]. A positive number indicates a positive correlation between the parameter and the state variable, while a negative number is an indication of negative correlation [*Gbondo-Tugbawa et al.*, 2001; *Jørgensen*, 1988]. The range of maximum and minimum temperature, precipitation, and PAR used for this analysis was determined from long-term measurements at the HBEF. Climatic input values included: the warmest and coolest year, wettest and driest year, and maximum and minimum long-term annual PAR values. In each model run, all other inputs and parameters were held constant, while varying only one maximum or minimum value for the input of interest (total of six runs).

3. Results

3.1. Model Performance

[17] The predicted annual streamflow over the measurement period of 1964–2008 generally matched observed values, with the exception of 1973, 1990, and 1996, which are the three highest annual discharge years on record and were underpredicted by the model (NME = –0.02, NMAE = 0.07; see Table 1 and Figure 1a). A long-term increase in discharge at the HBEF is consistent with a pattern of

[1] Auxiliary materials are available in the HTML. doi:10.1029/2011WR011228.

Table 1. Summary of Annual Model Performance Metrics Normalized Mean Error (NME) and Normalized Mean Absolute Error (NMAE) Over the Period of 1964 to 2008

	Model Performance	
Simulated Constituent	NME	NMAE
Stream flow	−0.02	0.07
SO_4^{2-}	0.03	0.06
NO_3^- (1964–1990)	1.17 (0.12)	1.38 (0.36)
Ca^{2+}	<0.01	0.19
Mg^{2+}	0.05	0.12
K^+	<0.01	0.16
Na^+	0.03	0.09
DOC	0.03	0.14
pH	<−0.01	0.02
ANC	4.24	−4.24

increasing precipitation [*Campbell et al.*, 2011]. The seasonal variation in streamflow matched observed values reasonably well (Table 2), although there was variability in model performance metrics over different seasons with minimum (NMAE = 0.19) and maximum (NMAE = 0.31) discrepancies over spring (April–June) and winter (January–March), respectively. The model slightly underpredicted spring (NME = –0.08) and winter (NME = –0.07) stream discharge while slightly overpredicting summer (July–September) (NME = 0.07) and fall (October–December) (NME = 0.06) streamflow (Table 2).

[18] The model generally captured the long-term trend of decreasing $(SO)_4^{2-}$ concentration and showed little overprediction (NME = 0.03, NMAE = 0.06; see Table 1 and Figure 1b). The model reproduced the long-term pattern of stream NO_3^- concentration until ~1990 (1964–1990; NME = 0.12, NMAE = 0.36; see Table 1 and Figure 1c), after which the model overpredicted measured NO_3^-, resulting in poorer model performance compared to SO_4^{2-} over the record (NME = 1.17, NMAE = 1.38; see Table 1).

[19] Stream Ca^{2+} was somewhat underpredicted by the model during the beginning of the record (Figure 1d), especially the peak in 1970, and overpredicted during the latter part of the record. However, overall, the model sufficiently captured the declining trend of observed Ca^{2+} values (NME < 0.01, NMAE = 0.19; see Table 1). The model also simulated stream concentrations of Mg^{2+} (NME = 0.05, NMAE = 0.12; see Table 1), K^+ (NME < 0.01, NMAE = 0.16; see Table 1) and Na^+ (NME = 0.03, NMAE = 0.09; see Table 1) reasonably well.

[20] Measured stream water concentrations of dissolved organic carbon (DOC) are available from 1982 (Figure 1e). The simulated annual volume-weighted average concentration of DOC in stream water depicted the measured values reasonably well (NME = 0.03, NMAE = 0.14; see Table 1). The long-term average DOC concentration produced by the model was 167 μmol C L^{-1}, which was comparable to the measured value of 162 μmol C L^{-1}.

[21] The model also captured the trend in stream water pH but slightly underpredicted values (NME < –0.01, NMAE = 0.02; see Table 1 and Figure 1f). The model also underpredicted ANC values (NME = 4.24, NMAE = –4.24; see Table 1). The average of the simulated and measured stream water ANC is –12.7 and –2.4 μeq L^{-1}, respectively. The underpredictions in stream pH and ANC are consistent with the overprediction of NO_3^- in recent years. Simulated soil base saturation was 10%, which is comparable to a field value of 9.5% measured in 1983 by *Johnson et al.* [1991].

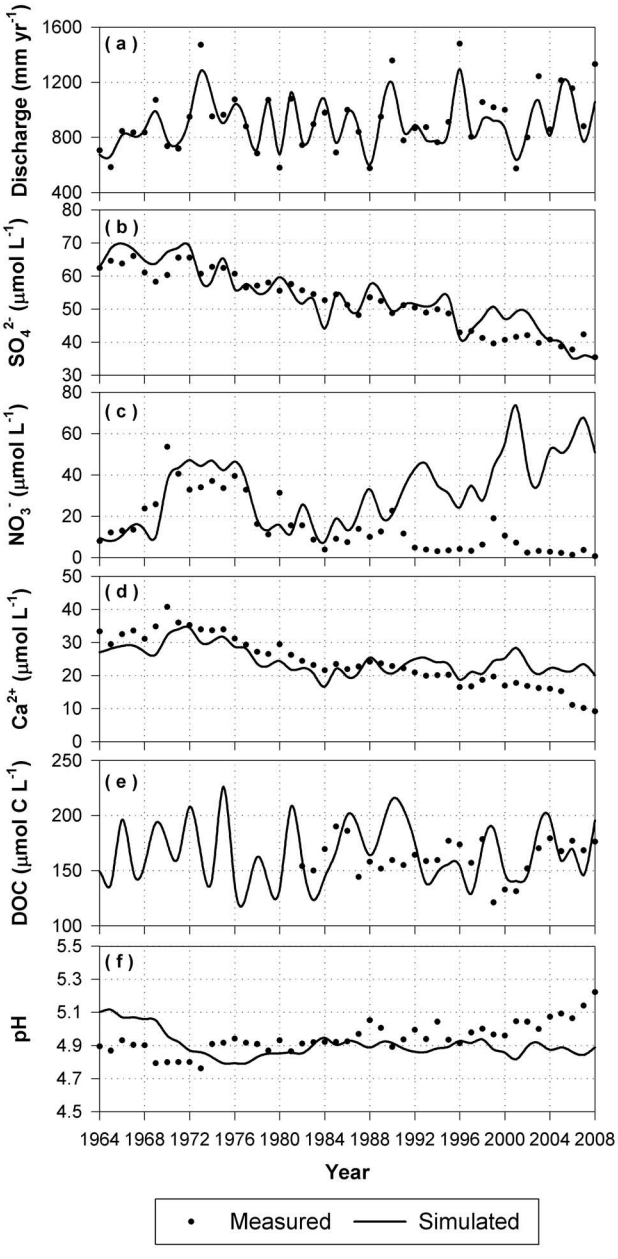

Figure 1. A comparison of measured and simulated values of (a) annual discharge and annual volume-weighted concentrations of (b) SO_4^{2-}, (c) NO_3^-, (d) Ca^{2+}, (e) DOC, and (f) stream water pH over the period 1964–2008 at watershed 6 of the Hubbard Brook Experimental Forest, N. H.

3.2. Sensitivity Analysis

[22] The selected state variables showed the greatest response to variations in temperature and PAR (Table 3). Higher temperatures increased model predictions of NO_3^- and DOC concentrations and decreased discharge, ANC,

Table 2. Summary of Annual and Seasonal Streamflow Model Performance Metrics Normalized Mean Error (NME) and Normalized Mean Absolute Error (NMAE) Over the Period of 1964 to 2008

	Model Performance	
Period	NME	NMAE
Annual	−0.02	0.07
Spring	−0.08	0.19
Summer	0.07	0.29
Fall	0.06	0.20
Winter	−0.07	0.31

and soil BS%. The sensitivity analysis also suggested that higher annual precipitation decreased NO_3^- and DOC concentrations and soil BS%, while increasing ANC. Higher PAR values resulted in a decrease in discharge and NO_3^- concentrations and increased DOC, ANC, and soil BS%. Precipitation had the greatest effect on discharge. The most sensitive state variable in this analysis was NO_3^-, which strongly influenced ANC and soil BS%. The least sensitive state variable was DOC, which was most dependent on temperature.

3.3. Future Climatic Projections

[23] The average measured temperature for HBEF is 5.7 (°C) (station 1: 1955–2008). Statistically downscaled AOGCM climate projections for the HBEF indicated increases in average air temperature of 1.7°C to 6.5°C by the end of the century, depending on the AOGCM and greenhouse gas emission trajectory selected (Table 4). The greatest temperature increase was projected by HadCM3-A1fi, while PCM-B1 showed the most modest increase. Precipitation projections were highly variable, ranging from 4 to 32 cm above the long-term annual measured average of 144 cm. Long-term annual average PAR at the HBEF is 566 mmol m^{-2} s^{-1}, and the climate projections indicate changes ranging from –26.7 to 143.1 mmol m^{-2} s^{-1} by 2100 depending on the scenario and model considered.

3.4. Hydrology

[24] Based on PnET-BGC model results, climate change is projected to cause substantial temporal shifts in hydrologic patterns at the HBEF (Figure 2). Modeling results indicate that spring (April–June) snowmelt will occur earlier and will be less extreme in the future. Low flows associated with enhanced evapotranspiration during the summer months (July–September), will extend earlier into the spring and later into the fall (October–December). Future streamflow in late fall and early winter (January–March) will increase because of less snowpack accumulation due to warmer air temperatures and concurrent declines in the ratio of snow to rain.

3.5. Soil and Stream Water Chemistry

[25] Model simulations showed that annual volume-weighted NO_3^- concentrations are projected to increase substantially over the next century under all six climate-change scenarios considered (Figures 3a and 4a, Table 5). Under HadCM3-A1fi, B1, and GFDL-A1fi, B1 scenarios, predicted annual volume-weighted NO_3^- concentration peaked around mid-century (2042, 2049, 2059, 2037, respectively) and then declined toward 2100 (see auxiliary material). In comparison, peaks in annual volume-weighted stream NO_3^- concentration under PCM-A1fi and B1 scenarios were delayed until later in the century. Average annual volume-weighted NO_3^- concentrations for the last 30 years of the twenty-first century are projected to range from 77 to 132 μmol L^{-1}, compared with an average annual observed value of 18 μmol L^{-1} for the past 30 years.

[26] The model projections for stream SO_4^{2-} showed a decline in concentration until ∼2025, and leveled off after that as the watershed approached steady state with respect to the business-as-usual scenario for atmospheric S deposition (Figures 3b and 4b). The average annual volume-weighted SO_4^{2-} concentration projected for 2070–2100 ranged from 23 to 27 μmol L^{-1}, which is lower than the average annual measured value of 53 μmol L^{-1} for the past 30 years.

[27] The model simulations of DOC showed that under all scenarios concentrations decreased over the next century (Figures 3c and 4c, Table 5). The average DOC concentrations projected for 2070–2100 range from 92 to 138 μmol C L^{-1}, which is somewhat lower than the mean annual measured value of 160 μmol C L^{-1} for 1982–2000.

[28] The model simulations for stream Ca^{2+} exhibited patterns that were correlated with changes in NO_3^- (Figures 3d and 4d). For the HadCM3 and GFDL simulations, annual volume-weighted Ca^{2+} concentrations increased until mid century, followed by a decline to the end of the century. Under the PCM simulations, stream Ca^{2+} remained constant until mid century and then increased in response to the later increase in NO_3^-. The average annual volume-weighted concentrations of Ca^{2+} for 2070–2100 ranged from 17 to 24 μmol L^{-1} (HadCM3-B1 and PCM-A1fi, respectively), which is comparable to the measured value of 25 μmol L^{-1} for 1970–2000. The soil BS% simulation reflected the stream NO_3^- and Ca^{2+} response, decreasing by almost 50% under the high temperature scenarios, while increasing slightly under lower temperature scenarios. The projected soil BS% for 2070–2100 ranged from 5.1% to 9.0%, in contrast to an average measured value of 9.5% [*Johnson et al.*, 1991].

[29] Future model projections of pH showed decreases under all scenarios (Figures 3e and 4e). The average annual volume-weighted pH projected for 2070–2100 ranged from 4.4 to 5.0, which encompasses the measured volume-weighted mean of 4.9 for 1970–2000. Depending on the

Table 3. Summary of Model Sensitivity Analysis to Changes in Temperature, Precipitation, and Photosynthetically Active Radiation (PAR)

Parameter	Range	$S^{Discharge}$	$S^{NO_3^-}$	S^{DOC}	S^{ANC}	$S^{\%BS}$
Temperature (°C)	4.46–7.22	−0.03	1.44	0.05	−1.29	−0.09
Precipitation (cm)	104.26–182.45	1.01	−0.51	−0.02	0.59	−0.02
PAR (mmol m^{-2} s^{-1})	456.15–629.99	−0.05	−1.43	0.04	1.25	0.24

Table 4. Summary of Climate Projections From Statistically Downscaled AOGCM Output[a]

	1970–2000	2070–2100					
		HadCM3		PCM		GFDL	
	Observed	A1fi	B1	A1fi	B1	A1fi	B1
Temperature (°C)	5.7	6.5	3.1	3.5	1.7	4.4	2.0
Annual precipitation (cm)	144	31.7	21.5	3.9	12.7	20.2	15.4
PAR (mmol m^{-2} s^{-1})	566	−4.6	41.2	104.7	143.1	17.2	−26.7

[a]The value shown for each scenario is the difference between the mean of measured values for the reference period 1970–2000 and the period 2070–2100.

scenario used, the acid-base response of the ecosystem to historic acidic deposition ranged from some recovery to no recovery. Acid neutralizing capacity (ANC) projections followed a similar pattern as pH. For the mean of 2070–2100 simulated ANC ranged from –9.5 to –42.2 μeq L^{-1}, which is less than the measured mean annual volume-weighted ANC of –3.4 μeq L^{-1} for 1988–2000.

[30] Annual element mass balances for each future climate change scenario were calculated to assess patterns in the fluxes and pools of major elements (NH_4^+ −N, NO_3^- −N, C, Ca^{2+}, Al) and associated processes depicted in PnET-BGC (Table 5). We summarized the PnET-BGC model results by calculating average output values using all six future climate-change scenarios. These average values were then used to examine the retention and loss of elements in the watershed over the period 2070–2100, and were compared with the average of simulated values for 1970–2000. The mass balances show that increases in stream water NO_3^- associated with higher temperature were mainly due to higher rates of N mineralization and nitrification. While NH_4^+ uptake by vegetation declined slightly, NO_3^- uptake greatly increased, resulting in an increase in total N assimilated by plants and a decrease in the pool of N in humus. Mobilization of Al from soil was enhanced due to acidification caused by high NO_3^- concentrations. Mineralization of carbon (C), without considering CO_2 effects on vegetation, decreased compared to the reference period, causing decreases in the humus C pool while the amount of C sequestrated in vegetation increased substantially. Uptake of Ca by vegetation declined, as did the humus and soil exchangeable pools; however, the total pool of Ca in plants increased.

3.6. Modeled CO_2 Effect

[31] Modeling results showed that the effect of increasing atmospheric CO_2 on vegetation had little impact on the seasonal distribution of stream discharge, causing only a slight increase in the quantity of streamflow during the growing season (Figure 2). A more detailed analysis of hydrologic responses to changes in climate and atmospheric CO_2 using PnET-BGC is given by *Campbell et al.* [2011].

[32] Compared to hydrology, including CO_2, effects on vegetation in the model had a more pronounced influence on stream NO_3^- concentrations, with substantially lower concentrations when CO_2 effects were considered (Figures 3a and 4a, Table 5). The results for model runs with CO_2 effects on vegetation, using the four lower and moderate scenarios of climate change (HadCM3-B1, GFDL-B1, PCM-A1fi, PCM-B1), indicated that the average annual volume-weighted NO_3^- concentration for the last 30 years of the twenty-first century ranged from 9 to 22 μmol L^{-1}, whereas NO_3^- concentrations for the two warmest scenarios (HadCM3-A1fi and GFDL-A1fi) were substantially higher (85 and 79 μmol L^{-1}, respectively). This differential response is due to a plateau in CO_2 fertilization that occurs at concentrations above 600 ppm, such that increased plant demand for N uptake is not able keep the pace with

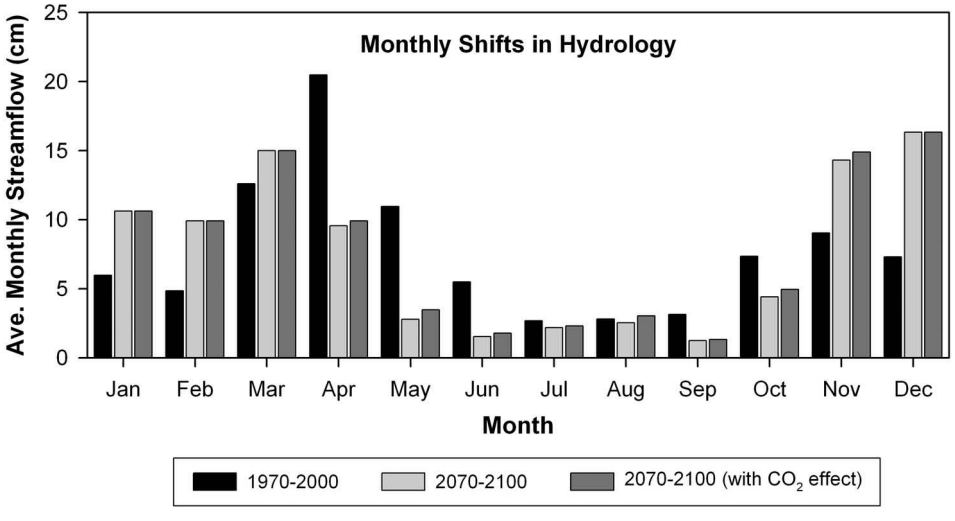

Figure 2. Comparison between measured monthly discharge for 1970–2000 and simulated mean monthly discharge for 2070–2100 with and without considering CO_2 effects on vegetation. Note the future climate-change scenario depicted in these results is from HadCM3 A1fi.

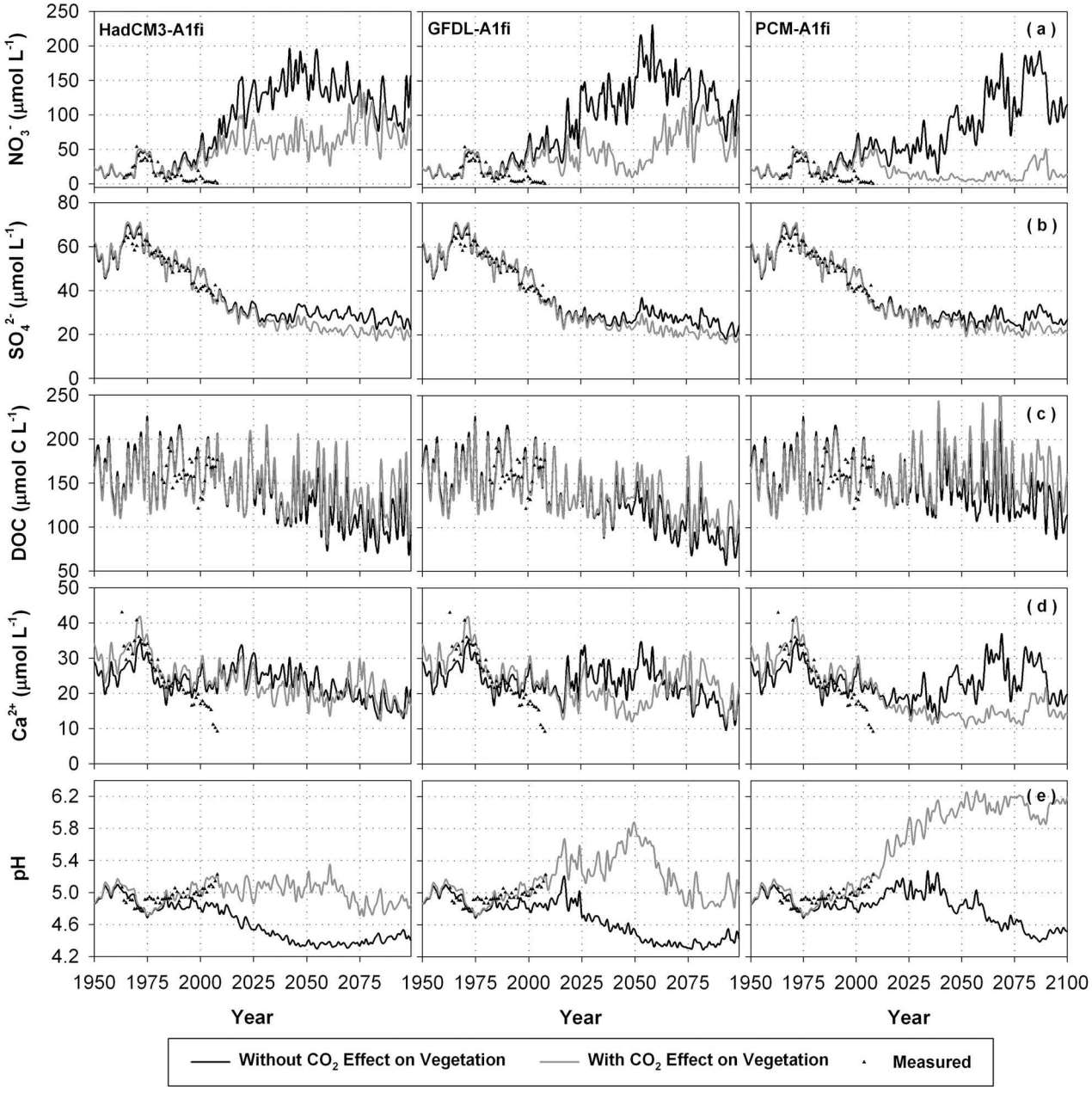

Figure 3. Past and future projections of annual volume-weighted concentrations of (a) NO_3^-, (b) SO_4^{2-}, (c) DOC, (d) Ca^{2+}, and (e) pH in stream water under A1fi scenarios with and without considering CO_2 effects on vegetation. Shown are measured data and simulations using input from three AOGCMs under high emission scenarios (A1fi).

increased available N pools from higher N mineralization associated with increasing temperature. In contrast to simulations of climate change, stream NO_3^- concentrations were lower under scenarios with the CO_2 effect on vegetation included. A condition of ecosystem N saturation was not as prominent, as elevated tree growth associated with CO_2 fertilization largely mitigated elevated NO_3^- losses.

[33] The model projections for stream Ca^{2+} concentration were lower when CO_2 effects were included in the model (Figures 3d and 4d, Table 5). Under the four lower and moderate climate scenarios (HadCM3-B1, GFDL-B1, PCM-A1fi, PCM-B1), the decline in the stream water Ca^{2+} concentration was due to enhanced uptake of Ca^{2+} by vegetation associated with CO_2 fertilization. Under the two warmest climate scenarios (HadCM3-A1fi and GFDL-A1fi), the peak in Ca^{2+} occurred later in response to elevated NO_3^-. The average annual volume-weighted concentration of Ca^{2+} for 2070–2100 for the four lower and moderate scenarios with CO_2 effects varied between 13 and 15 μmol L^{-1} compared to a measured mean value of 25 μmol L^{-1} for 1970–2000. The average annual volume-weighted Ca^{2+} concentrations for 2070–2100 for the warmest model simulations (HadCM3-A1fi and GFDL-A1fi) with CO_2 effects were 20 and 22 μmol L^{-1}, respectively.

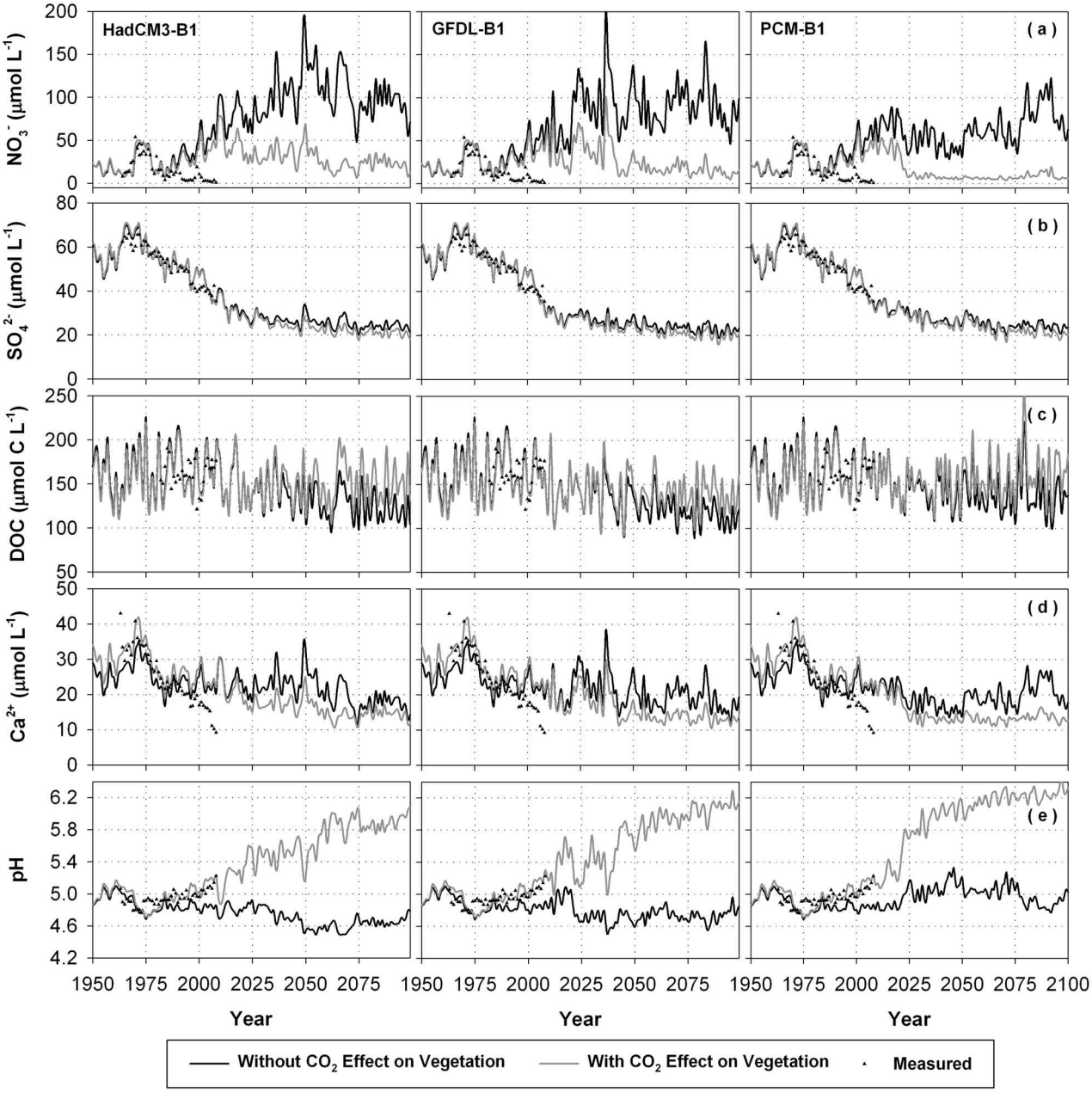

Figure 4. Past and future projections of annual volume-weighted concentrations of (a) NO_3^-, (b) SO_4^{2-}, (c) DOC, (d) Ca^{2+}, and (e) pH in stream water under B1 scenarios with and without considering CO_2 effects on vegetation. Shown are measured data and simulations using input from three AOGCMs under low emission scenarios (B1).

[34] Invoking CO_2 effects under climate change resulted in a change in the simulation of DOC loss (Figures 3c and 4c, Table 5). The simulated mean DOC concentrations for 2070–2100 were higher in comparison to values from model simulations without CO_2 effects on vegetation and exhibited an increased variation. The average DOC concentrations for the four lower and moderate scenarios with CO_2 effects on vegetation for 2070–2100 vary from 137 to 163 µmol C L^{-1}, while for the two warmest scenarios (HadCM3-A1fi and GFDL-A1fi) mean DOC concentrations were 126 and 112 µmol C L^{-1}, respectively.

[35] Future model projections of pH under the four lower and moderate scenarios of climate change with CO_2 effects showed recovery from the current conditions by up to 1 pH unit (steady state value ~6). The annual volume-weighted pH for the four low and moderate scenarios including CO_2 effects for 2070–2100 varied between 5.90 and 6.24, while pH values for the two warmest scenarios (HadCM3-A1fi and GFDL-A1fi) were considerably lower (4.84 and 4.95, respectively). Acid neutralizing capacity projections followed patterns similar to that of pH. The mean annual volume-weighted ANC for the four low and moderate scenarios of climate change with

Table 5. Projected Average Changes in Biogeochemical Fluxes (kg ha^{-1} yr^{-1}) and Pools (kg ha^{-1}) of Major Elements for the Hubbard Brook Experimental Forest[a]

Fluxes/Pools	NH_4–N			NO_3–N			C/DOC			Ca			Al		
Period	1970–2000	2070–2100[b]	2070–2100[c]	1970–2000	2070–2100[b]	2070–2100[c]	1970–2000	2070–2100[b]	2070–2100[c]	1970–2000	2070–2100[b]	2070–2100[c]	1970–2000	2070–2100[b]	2070–2100[c]
Deposition	2.4	2.0	2.0	5.6	2.5	2.5	17.2	20.0	20.0	1.6	1.8	1.8	0.2	0.3	0.3
Throughfall	2.0	1.6	1.6	5.6	2.5	2.5	17.2	20.0	20.0	3.5	2.0	2.0	0.2	0.3	0.3
Litterfall	93.6	86.8	95.1	0.0	0.0	0.0	6861	5543	6856	23.3	21.4	22.4	0.0	0.0	0.0
Weathering	0.0	0.0	0.0	0.0	0.0	0.0	0.0	0.0	0.0	3.8	3.8	4.8	4.5	4.5	4.5
Uptake	−82.5	−22.2	−71.9	−15.5	−69.0	−30.9	0.0	0.0	0.0	−39.5	−32.9	−34.3	0.0	0.0	0.0
Mineralization	94.2	99.9	103.5	13.7	79.3	33.2	5976	5109	6117	38.6	33.7	34.1	0.0	0.0	0.0
Nitrification	−13.7	−79.3	−33.2	13.7	79.3	33.2	0.0	0.0	0.0	0.0	0.0	0.0	0.0	0.0	0.0
Plant total	682	1036	1310	0.0	0.0	0.0	228,778	296,835	460,706	164	237	310	0.0	0.0	0.0
Humus	3372	2388	2620	0.0	0.0	0.0	119,713	79,138	91,332	666	443	432	0.0	0.0	0.0
Soil exchangeable pools	0.0	0.0	0.0	0.0	0.0	0.0	0.0	0.0	0.0	282	189	308	1663	1647	1679
Drainage losses	0.0	0.0	0.0	−3.8	−12.8	−4.8	−18.1	−11.9	−15.2	−9.7	−6.6	−5.9	−2.5	−3.9	−1.2

Note: Values for reference period of 1970–2000 are simulated values from PnET-BGC. Future values are the average output of all six climate scenarios over the period 2070–2100. Positive fluxes indicate an increase in soil solution concentration.

[a]Values are calculated as the difference between the mean for the period of 2070–2100 and the reference period of 1970–2000.

[b]Without CO_2 effects on vegetation.

[c]With CO_2 effects on vegetation.

CO_2 fertilization for 2070–2100 ranged from 6.9 to 15.5 μeq L^{-1}, in comparison with –3.4 μeq L^{-1} for mean annual measured values (for 1988–2000). Model simulations suggest that the mean annual volume-weighted ANC values for HadCM3-A1fi and GFDL-A1fi (the two warmest) were –13.6 and –10.5 μeq L^{-1}, respectively. Model outputs for soil %BS followed a similar pattern as NO_3^-, pH, and ANC. There was some increase in soil %BS under four moderate and low temperature scenarios, which ranged from 10.0% to 13.3% for the period of 2070–2100. The average %BS for the last 30 years of the twenty-first century produced by HadCM3-A1fi and GFDL-A1fi, however, were comparatively low (4.3 and 5.6, respectively). These results suggest that when CO_2 fertilization stimulates tree growth without elevated NO_3^- leaching, recovery from acidic deposition will occur, resulting in an increase in stream pH, ANC, and soil %BS. However, under the highest temperature scenarios (HadCM3-A1fi and GFDL-A1fi) enhanced mineralization of soil N and NO_3^- leaching reacidify soil and stream water.

[36] The model simulations indicated that climate change may alter the hydrologic cycle and the seasonality of stream discharge. Since drainage strongly influences element transport [*Likens and Bormann*, 1995] seasonal changes in discharge may also alter the seasonal patterns of chemical constituents. We assessed changes in seasonal patterns of concentrations of NO_3^-, Ca^{2+}, pH, and ANC under all climate-change scenarios with and without CO_2 effects on vegetation over the period of 2070–2100 and compared these with the seasonal patterns of measured values from 1970–2000. The timing, patterns, and magnitude of stream water NO_3^- concentrations are highly variable depending on the climate scenarios used (see auxiliary material). Since NO_3^- is the main driver of acid-base status of the ecosystem, Ca^{2+}, pH, and ANC follow similar patterns. These results suggest that as climate change will likely alter the overall element concentrations and fluxes, these changes will be manifested in the seasonal patterns of elements concentrations and fluxes and the timing of these changes.

[37] Element mass balances showed that when CO_2 effects were included, the uptake of NH_4^+ by vegetation increased and exceeded the uptake of NO_3^-. Also, the amount of total N sequestrated in plants increased, which was followed by an increase in N in litterfall and the humus pool. Nitrification rates decreased compared with values without considering CO_2 effects, causing less NO_3^- leaching. Carbon sequestration by plants increased, which was followed by an increase in litterfall, the humus pool, and the mineralization of organic C, ultimately resulting in increases in stream water DOC. The amount of Ca^{2+} sequestrated in plants increased, which was followed by an increase in litterfall and the mineralization of Ca^{2+}. Pools of exchangeable Ca^{2+} in soil also increased due to lower concentrations of NO_3^-.

4. Discussion

4.1. Model Performance

[38] Overall, the model performed well and adequately simulated the observed values. The model satisfactorily captured seasonal variation in streamflow patterns, with slight overprediction during summer and fall, and slight

underprediction during spring and winter. These over- and underpredictions are manifested in a slight underprediction of annual discharge. Therefore, the model captured the general annual hydrologic pattern over the period of 1964–2008 without any tendency in over- or underprediction.

[39] Although there was a slight overprediction of stream SO_4^{2-}, the model captured the long-term trend of decreasing SO_4^{2-} concentration. This long-term decline in stream SO_4^{2-} is due to emission controls of SO_2 associated with the 1970 and 1990 Amendments to the Clean Air Act [*Driscoll et al.*, 2001]. In general, the model overpredicted NH_4^+ concentrations. Because of the low selectivity coefficient for soil-NH_4^+ exchange (Log $K = -0.107$) [*Gbondo-Tugbawa et al.*, 2001], the exchangeable pool of NH_4^+ is very small. The higher simulated concentration of NH_4^+ and subsequent increase in soil pools triggered higher rates of nitrification and soil N mineralization, which contributed to the overprediction of NO_3^- in stream water. There has been an unexplained decline in measured stream NO_3^- concentrations at the HBEF and surrounding region despite a high chronic atmospheric deposition of N and the increasing age of the forest [*Goodale et al.*, 2003, 2005] which is consistent with an overprediction of simulated stream NO_3^- concentrations. Modeling the N cycle in forest ecosystems is a challenge due to complexity, confounding factors, and limitations in knowledge about the N cycle in forest ecosystems, hampering the development of algorithms in the model that enable adequate depiction of stream water N losses. PnET-BGC incorporates current thinking of the nitrogen cycle of forest ecosystems to the extent that we understand it, but until a mechanism for the decrease in N loss can be identified and quantified it seems dishonest to modify an input or parameter of the model or invoke a poorly understood process to fit the measured data. Nevertheless, PnET-BGC is effective in simulating the response of the N to vegetation disturbance [*Aber et al.*, 2002] and so likely captures the plant-soil perturbation associated with changing climate.

[40] The model calculates pH from a charge balance of all ions in stream water and mass law expressions of dissolved inorganic carbon, Al, and natural occurring organic acids [*Gbondo-Tugbawa et al.*, 2001]. Accurate modeling of pH is a key component in most watershed models which simulate acid-base chemistry because many biological processes and effects are closely linked with pH [*Gbondo-Tugbawa et al.*, 2001]. Simulation of pH is especially challenging in systems with ANC values close to 0 $\mu eq\ L^{-1}$, like the HBEF (pH 4.7–5.7) [*Davis et al.*, 1987]. Since pH values are affected by all biogeochemical processes which influence the concentrations of ionic solutes, slight errors in the simulation of major elements can result in high variation and possible errors in pH predictions. Based on model performance criteria for pH, slight overprediction of SO_4^{2-} and NO_3^- are compensated for, to some extent, by slight an overprediction of base cations. The underprediction of ANC values are mainly due to overprediction of NO_3^- and naturally occurring organic acids (i.e., DOC).

4.2. Sensitivity Analysis

[41] The sensitivity analysis showed that state variables were most responsive to variations in temperature and PAR. Higher temperatures resulted in higher rates of mineralization and nitrification, causing a higher NO_3^- concentration and lower ANC in stream water and lower soil %BS. Higher PAR results in higher rates of photosynthesis and greater plant uptake of nutrients, especially N, causing lower surface water NO_3^- and higher values of ANC and soil %BS. Also, higher photosynthesis and the associated increase in vegetation growth and litterfall led to the projected increase in DOC. DOC was most sensitive to temperature since it is a by-product of organic carbon mineralization. Stream water discharge showed a high dependency on precipitation. The results of this sensitivity analysis coupled with the previous sensitivity analysis of PnET-BGC inputs and parameters [*Gbondo-Tugbawa et al.*, 2001] show that model predictions are relatively sensitive to changes in climate, indicating that future climate change will likely elicit a marked hydrochemical response in temperate forest watersheds.

4.3. Modeling Results for Hydrology, Soil, and Stream Water Chemistry

[42] Under PnET-BGC model runs without CO_2 effects, warmer temperatures in the future caused a decrease in soil moisture and an increase in vapor pressure deficit, despite the increase in precipitation. These factors decrease evapotranspiration and cause midsummer drought stress, the extent of which is dependent on the climate-change scenario considered. Although wood net primary production (NPP) increased due to warmer temperatures and a longer growing season, repeated midsummer drought is projected to decrease maximum leaf area index, foliar NPP, and litterfall and fine root NPP [*Aber and Federer*, 1992; *Campbell et al.*, 2009, 2011] (Table 5). Overall, these changes translate into less C sequestration in foliage and fine roots, and more in wood. Because of slower decomposition rates associated with woody litter, the model simulates a decrease in C transfer to humus. The increase in wood NPP does not offset the decline in the litter inputs (sum of leaf litterfall and fine roots) to the soil organic matter (SOM) pool.

[43] The assimilation of N, Ca, and other nutrients in plant tissues was similar to the pattern for C. The result of the shift in NPP was a decrease in litterfall elements, causing declines in the humus pool (Table 5). Because of water stress, the plant demand for N decreased and the available N pool for plants increased, resulting in a 6.6% decrease in the C:N ratio of the humus pool (Table 5). Although both model simulations and observed values show that the HBEF is currently a sink for atmospheric N deposition, future model simulations suggest that climate change may cause the site to shift to N source to downstream aquatic ecosystems. Note that previous experiments and measurements at the HBEF have demonstrated that the N cycle is very sensitive to ecosystem disturbance that affects forest vegetation [*Likens et al.*, 1970; *Houlton et al.*, 2003].

[44] The elevated export of NO_3^- from forest soils to surface waters is an environmental concern in the northeastern U. S. and elsewhere [*Aber et al.*, 2003; *Driscoll et al.*, 2003]. Elevated leaching losses of NO_3^- facilitate the depletion of cations from soil, and contribute to soil and surface water acidification [*Driscoll et al.*, 2003]. High NO_3^- can lead to water quality impairments and can contribute to the eutrophication of coastal waters. It is challenging to model N losses from forest ecosystems, due to a poor understanding of processes that control N cycling, particularly those

associated with immobilization and denitrification [e.g., *Dail et al.*, 2001; *Venterea et al.*, 2004]. Nitrogen retention is sensitive to a variety of factors, including the legacy effects of historical land use and disturbance which are often poorly characterized [*Aber et al.*, 2002]. Despite these uncertainties, PnET-BGC is a useful tool for assessing the effects of climate change on the N cycle since it accounts for other disturbances including climate change, N deposition, and atmospheric CO_2 simultaneously [*Ollinger et al.*, 2009].

[45] For model runs that did include CO_2 effects, plant WUE increased and midsummer drought did not occur appreciably except under the two warmest scenarios (HadCM3-A1fi and GFDL-A1fi). The effect of elevated CO_2 on stomatal conductance and the increase in WUE offset the effect of higher temperatures by enhanced tree growth and higher nutrient uptake. Over the second half of the century under the two warmest scenarios (HadCM3-A1fi and GFDL-A1fi), the CO_2 effect on vegetation was not able to offset the effect of temperature; midsummer droughts and water stress caused less uptake of N and the elevated availability of N followed by nitrification and elevated leachate of NO_3^-. Increases in atmospheric CO_2 resulted in increased tree growth and limited NO_3^- leaching over the first half of the twenty-first century, while tree growth remained constant or decreased over the second half of the century because of water stress. This pattern is due to the nonlinear response of photosynthesis to increasing atmospheric CO_2. Over time, and especially under higher CO_2 emission scenarios and warmer temperatures, the CO_2 fertilization effect declines and N saturation occurs, as temperature becomes the dominant driver of N cycling. This work suggests that the legacy of an accumulation of elevated N deposition in forest watersheds downwind of emission sources could have delayed deleterious effects on soil and surface water. If stores of N are mineralized under changing climate, the consequences of elevated NO_3^- leaching could be realized. In this study, we assumed that N emissions remained at current levels and did not consider future land disturbances in our simulations. If atmospheric N deposition decreases or land disturbance occurs in the future, N saturation would be delayed.

[46] Studies suggest that surface water DOC is increasing in Europe and the northeastern U. S. The alternative mechanisms explaining this phenomenon are declines in acidic deposition or climate change [*Clark et al.*, 2010; *Evans et al.*, 2006; *Findlay*, 2005; *Freeman et al.*, 2001, 2004; *Garnett et al.*, 2000; *Monteith et al.*, 2007; *Worrall et al.*, 2003]. PnET-BGC simulations suggest that DOC will decrease over the twenty-first century under all climate-change scenarios. This modeled decline in DOC is associated with a decline in litterfall and a decrease in soil C mineralization rates (Table 5). The trends in stream water DOC were modified under climate change in the presence of CO_2 fertilization. The higher productivity of the forest (NPP and net ecosystem production) due to CO_2 fertilization increased litterfall in comparison to values from model simulations without CO_2 effects on vegetation (Table 5). An increase in the decomposition of the organic matter pool, triggered by higher temperatures, led to higher DOC concentrations in stream water. Note that when CO_2 effects on vegetation were included in the simulations, large increases in stream DOC were not evident. Our model simulations would seem to be inconsistent with the hypothesis that climate change is driving increases in surface water DOC.

[47] While hydrochemical models such as PnET-BGC provide useful information about how ecosystems may respond to global change, they are somewhat limited by sources of uncertainty. First, there are only a few studies that have evaluated the effects of CO_2 fertilization on NPP, especially in northern hardwood forest ecosystems [*Ainsworth and Long*, 2005; *Curtis and Wang*, 1998; *Curtis et al.*, 1995; *Ellsworth*, 1999; *Ellsworth et al.*, 1995; *Lewis et al.*, 1996; *Saxe et al.*, 1998]. Experimental manipulations show that increased atmospheric CO_2 enhances plant productivity, but the extent of this response over the long term in conjunction with other global-change drivers is not well established. Second, it is unclear how atmospheric deposition will change in the future, which could substantially influence the element responses. Moreover, we did not consider scenarios of future land disturbance, which could further affect hydrologic and biogeochemical dynamics. Third, changes in climate and other factors (e.g., pests, pathogens) may alter the composition of vegetation at the HBEF, which could also influence hydrologic (e.g., transpiration) and biogeochemical (e.g., uptake, litterfall, decomposition) fluxes. While changes in established tree species would occur slowly in response to climate change, the effects might be more pronounced at locations such as the HBEF, which are located in a transition forest zone (between northern hardwoods and red spruce-balsam fir forests). In this application, PnET-BGC model simulations assumed that the watershed consisted of a homogeneous distribution of northern hardwood forest. In the future it would be useful to evaluate the influence of shifts in species composition or to link PnET-BGC with a forest community model that projects changes species assemblages. The temperature conditions considered in some of the climate scenarios are beyond the conditions under which parameter values were developed for PnET-BGC. We are currently evaluating model performance for watersheds of lower latitude to assess this limitation. Finally, it is important to reduce the uncertainty of climate-change projections, particularly for precipitation, by continuing to improve climate models, downscaling techniques (e.g., station-based instead of gridded), and linkages with hydrochemical models.

5. Conclusions

[48] In this study we evaluated the hydrochemical response of a northern hardwood forest watershed to projected changes in climate and atmospheric CO_2. A sensitivity analysis showed that model output was sensitive to climatic drivers that are changing and are expected to change more in the upcoming decades (temperature, precipitation, solar radiation). As model calculations suggest that under changes in climate that induce water stress (decreases in summer soil moisture due to shifts in hydrology and increased evapotranspiration), an uncoupling of plant element cycling results in conditions of net mineralization/nitrification and soil and water acidification. Forest fertilization associated with increases in CO_2 appears to mitigate this perturbation somewhat. Moving forward, there is a critical need to better understand the interplay among multiple disturbances and the legacies of these ecosystems in order to project their response to global change.

[49] **Acknowledgments.** The authors would like to thank the three anonymous reviewers for providing helpful comments that improved this manuscript. Funding for this study was provided by the Environmental Protection Agency and the USDA Northeastern States Research Cooperative. This manuscript is a contribution of the Hubbard Brook Ecosystem Study. Hubbard Brook is part of the Long-Term Ecological Research (LTER) network, which is supported by the National Science Foundation. The Hubbard Brook Experimental Forest is operated and maintained by the USDA Forest Service, Northern Research Station, Newtown Square, PA.

References

Aber, J. D., and C. T. Driscoll (1997), Effects of land use, climate variation, and N deposition on N cycling and C storage in northern hardwood forests, *Global Biogeochem. Cycles*, *11*(4), 639–648, doi:10.1029/97GB01366.

Aber, J. D., and C. A. Federer (1992), A generalized, lumped-parameter model of photosynthesis, evapotranspiration and net primary production in temperate and boreal forest ecosystems, *Oecologia*, *92*(4), 463–474, doi:10.1007/BF00317837.

Aber, J. D., S. V. Ollinger, C. A. Federer, P. B. Reich, M. L. Goulden, D. W. Kicklighter, J. M. Melillo, and R. G. Lathrop Jr. (1995), Predicting the effects of climate change on water yield and forest production in the northeastern United States, *Clim. Res.*, *05*(3), 207–222, doi:10.3354/cr0005207.

Aber, J. D., P. B. Reich, and M. L. Goulden (1996), Extrapolating leaf CO_2 exchange to the canopy: A generalized model of forest photosynthesis compared with measurements by eddy correlation, *Oecologia*, *106*(2), 257–265, doi:10.1007/BF00328606.

Aber, J. D., S. V. Ollinger, and C. T. Driscoll (1997), Modeling nitrogen saturation in forest ecosystems in response to land use and atmospheric deposition, *Ecol. Modell.*, *101*(1), 61–78, doi:10.1016/S0304-3800(97)01953-4.

Aber, J. D., S. V. Ollinger, C. T. Driscoll, G. E. Likens, R. T. Holmes, R. J. Freuder, and C. L. Goodale (2002), Inorganic nitrogen losses from a forested ecosystem in response to physical, chemical, biotic, and climatic perturbations, *Ecosystems*, *5*(7), 648–658, doi:10.1007/s10021-002-0203-2.

Aber, J. D., C. L. Goodale, S. V. Ollinger, M. Smith, A. H. Magill, M. E. Martin, R. A. Hallett, and J. L. Stoddard (2003), Is nitrogen deposition altering the nitrogen status of northeastern forests? *BioScience*, *53*(4), 375–389, doi:10.1641/0006-3568(2003)053[0375:INDATN]2.0.CO;2.

Ainsworth, E. A., and S. P. Long (2005), What have we learned from 15 years of free-air CO_2 Enrichment (FACE)? A meta-analytic review of the responses of photosynthesis, canopy properties and plant production to rising CO_2, *New Phytologist*, *165*(2), 351–371, doi:10.1111/j.1469-8137.2004.01224.x.

Ainsworth, E. A., and A. Rogers (2007), The response of photosynthesis and stomatal conductance to rising [CO_2]: Mechanisms and environmental interactions, *Plant Cell Environ.*, *30*(3), 258–270, doi:10.1111/j.1365-3040.2007.01641.x.

Ainsworth, E. A., P. A. Davey, G. J. Hymus, B. G. Drake, and S. P. Long (2002), Long-term response of photosynthesis to elevated carbon dioxide in a Florida scrub-oak ecosystem, *Ecol. Appl.*, *12*(5), 1267–1275.

Beerling, D. J. (1996), Ecophysiological responses of woody plants to past CO_2 concentrations, *Tree Physiol.*, *16*(4), 389–396, doi:10.1093/treephys/16.4.389.

Campbell, J., et al. (2009), Consequences of climate change for biogeochemical cycling in forests of northeastern North America, *Can. J. Forest Res.*, *39*(2), 264–284, doi:10.1139/X08-104.

Campbell, J. L., C. T. Driscoll, A. Pourmokhtarian, and K. Hayhoe (2011), Streamflow responses to past and projected future changes in climate at the Hubbard Brook Experimental Forest, New Hampshire, United States, *Water Resour. Res.*, *47*, W02514, doi:10.1029/2010WR009438.

Chen, L., and C. T. Driscoll (2005), A two-layer model to simulate variations in surface water chemistry draining a northern forest watershed, *Water Resour. Res.*, *41*(9), W09425, doi:10.1029/2004WR003625.

Clark, J., S. Bottrell, C. Evans, D. Monteith, R. Bartlett, R. Rose, R. Newton, and P. Chapman (2010), The importance of the relationship between scale and process in understanding long-term DOC dynamics, *Sci. Total Environ.*, *408*(13), 2768–2775, doi:10.1016/j.scitotenv.2010.02.046.

Curtis, P. S., and X. Wang (1998), A meta-analysis of elevated CO_2 effects on woody plant mass, form, and physiology, *Oecologia*, *113*(3), 299–313, doi:10.1007/s004420050381.

Curtis, P. S., C. S. Vogel, K. S. Pregitzer, D. R. Zak, and J. A. Teeri (1995), Interacting effects of soil fertility and atmospheric CO_2 on leaf area growth and carbon gain physiology in *Populus x euramericana* (Dode) Guinier, *New Phytologist*, *129*(2), 253–263, doi:10.1111/j.1469-8137.1995.tb04295.x.

Dail, D., E. Davidson, and J. Chorover (2001), Rapid abiotic transformation of nitrate in an acid forest soil, *Biogeochemistry*, *54*(2), 131–146, doi:10.1023/A:1010627431722.

Davis, G., J. Whipple, S. Gherini, C. Chen, R. Goldstein, A. Johannes, P. Chan, and R. Munson (1987), Big Moose Basin: Simulation of response to acidic deposition, *Biogeochemistry*, *3*(1), 141–161, doi:10.1007/BF02185190.

Delworth, T. L., et al. (2006), GFDL's CM2 global coupled climate models. Part I: Formulation and simulation characteristics, *J. Clim.*, *19*(5), 643–674, doi:10.1175/JCLI3629.1.

Drake, B. G., M. A. Gonzalez-Meler, and S. P. Long (1997), More efficient plants: A consequence of rising atmospheric CO_2?, *Annu. Rev. Plant. Physiol. Plant. Mol. Biol.*, *48*(1), 609–639, doi:10.1146/annurev.arplant.48.1.609.

Driscoll, C. T., G. B. Lawrence, A. J. Bulger, T. J. Butler, C. S. Cronan, C. Eagar, K. F. Lambert, G. E. Likens, J. L. Stoddard, and K. C. Weathers (2001), Acidic deposition in the northeastern United States: Sources and inputs, ecosystem effects, and management strategies, *BioScience*, *51*(3), 180–198, doi:10.1641/0006-3568(2001)051[0180:ADITNU]2.0.CO;2.

Driscoll, C. T., et al. (2003), Nitrogen pollution in the northeastern United States: Sources, effects, and management options, *Bioscience*, *53*(4), 357–374, doi:10.1641/0006-3568(2003)053[0357:NPITNU]2.0.CO;2.

Ellsworth, D. S. (1999), CO_2 enrichment in a maturing pine forest: Are CO_2 exchange and water status in the canopy affected?, *Plant Cell Environ.*, *22*, 461–472, doi:10.1046/j.1365-3040.1999.00433.x.

Ellsworth, D. S., R. Oren, C. Huang, N. Phillips, and G. R. Hendrey (1995), Leaf and canopy responses to elevated CO_2 in a pine forest under free-air CO_2 enrichment, *Oecologia*, *104*(2), 139–146, doi:10.1007/BF00328578.

Evans, C., P. Chapman, J. Clark, D. Monteith, and M. Cresser (2006), Alternative explanations for rising dissolved organic carbon export from organic soils, *Global Change Biol.*, *12*, 2044–2053, doi:10.1111/j.1365-2486.2006.01241.x.

Farquhar, G., and S. Wong (1984), An empirical model of stomatal conductance, *Functional Plant Biol.*, *11*(3), 191–210.

Findlay, S. E. G. (2005), Increased carbon transport in the Hudson River: Unexpected consequence of nitrogen deposition? *Frontiers Ecol. Environ.*, *3*(3), 133–137.

Freeman, C., C. D. Evans, D. T. Monteith, B. Reynolds, and N. Fenner (2001), Export of organic carbon from peat soils, *Nature*, *412*(6849), 785, doi:10.1038/35090628.

Freeman, C., N. Fenner, N. J. Ostle, H. Kang, D. J. Dowrick, B. Reynolds, M. A. Lock, D. Sleep, S. Hughes, and J. Hudson (2004), Export of dissolved organic carbon from peatlands under elevated carbon dioxide levels, *Nature*, *430*(6996), 195–198, doi:10.1038/nature02707.

Garnett, M. H., P. Ineson, and A. C. Stevenson (2000), Effects of burning and grazing on carbon sequestration in a Pennine blanket bog, UK, *Holocene*, *10*(6), 729–736, doi:10.1191/09596830094971.

Gbondo-Tugbawa, S. S., C. T. Driscoll, J. D. Aber, and G. E. Likens (2001), Evaluation of an integrated biogeochemical model (PnET-BGC) at a northern hardwood forest ecosystem, *Water Resour. Res.*, *37*(4), 1057–1070, doi:10.1029/2000WR900375.

Goodale, C. L., J. D. Aber, and P. M. Vitousek (2003), An unexpected nitrate decline in New Hampshire streams, *Ecosystems*, *6*(1), 0075–0086, doi:10.1007/s10021-002-0219-0.

Goodale, C. L., J. D. Aber, P. M. Vitousek, and W. H. McDowell (2005), Long-term decreases in stream nitrate: Successional causes unlikely; possible links to DOC? *Ecosystems*, *8*(3), 334–337, doi:10.1007/s10021-003-0162-8.

Hayhoe, K., et al. (2004), Emissions pathways, climate change, and impacts on California, *Proc. Natl. Acad. Sci. U. S. A.*, *101*(34), 12422–12427, doi:10.1073/pnas.0404500101.

Hayhoe, K., et al. (2007), Past and future changes in climate and hydrological indicators in the US northeast, *Clim. Dyn.*, *28*(4), 381–407, doi:10.1007/s00382-006-0187-8.

Hayhoe, K., C. Wake, B. Anderson, X. Liang, E. Maurer, J. Zhu, J. Bradbury, A. DeGaetano, A. Stoner, and D. Wuebbles (2008), Regional climate change projections for the northeast USA, *Mitigation and Adaptation Strategies for Global Change*, *13*(5), 425–436, doi:10.1007/s11027-007-9133-2.

Houlton, B. Z., C. T. Driscoll, T. J. Fahey, G. E. Likens, P. M. Groffman, E. S. Bernhardt, and D. C. Buso (2003), Nitrogen dynamics in ice storm-damaged forest ecosystems: Implications for nitrogen limitation theory, *Ecosystems*, *6*(5), 431–443, doi:10.1007/s10021-002-0198-1.

Intergovernmental Panel on Climate Change (IPCC) (2007), Climate change 2007: The physical science basis, contribution of Working Group

I to *The Fourth Assessment Report of the Intergovernmental Panel on Climate Change*, edited by S. Solomon et al., Cambridge Univ. Press, Cambridge, U. K., 996 pp.

Janssen, P. H. M., and P. S. C. Heuberger (1995), Calibration of process-oriented models, *Ecol. Modell.*, *83*(1–2), 55–66, doi:10.1016/0304-3800(95)00084-9.

Jarvis, A. J., and W. J. Davies (1998), The coupled response of stomatal conductance to photosynthesis and transpiration, *J. Exp. Bot.*, *49*, 399–406, doi:10.1093/jxb/49.Special_Issue.399.

Johnson, C. E., A. H. Johnson, and T. G. Siccama (1991), Whole-tree clear-cutting effects on exchangeable cations and soil acidity, *Soil Sci. Soc. Am. J.*, *55*(2), 502–508, doi:10.2136/sssaj1991.03615995005500020035x.

Johnson, C. E., C. T. Driscoll, T. G. Siccama, and G. E. Likens (2000), Element fluxes and landscape position in a northern hardwood forest watershed ecosystem, *Ecosystems*, *3*(2), 159–184, doi:10.1007/s100210000017.

Jørgensen, S. E. (1988), *Fundamentals of Ecological Modeling, Developmentes in Environmental Modeling*, 628 pp., Elsevier, N. Y.

Lewis, J. D., D. T. Tissue, and B. R. Strain (1996), Seasonal response of photosynthesis to elevated CO_2 in loblolly pine (*Pinus taeda L.*) over two growing seasons, *Global Change Biol.*, *2*(2), 103–114, doi:10.1111/j.1365-2486.1996.tb00055.x.

Liang, X., D. P. Lettenmaier, E. F. Wood, and S. J. Burges (1994), A simple hydrologically based model of land surface water and energy fluxes for general circulation models, *J. Geophys. Res.*, *99*(D7), 14415–14428, doi:10.1029/94JD00483.

Likens, G. E., and F. H. Bormann (1995), *Biogeochemistry of a Forested Ecosystem*, 2nd ed., 159 pp., Springer, N. Y.

Likens, G. E., F. H. Bormann, N. M. Johnson, D. W. Fisher, and R. S. Pierce (1970), Effects of forest cutting and herbicide treatment on nutrient budgets in the Hubbard Brook watershed-ecosystem, *Ecol. Monogr.*, *40*(1), 23–47, doi:10.2307/1942440.

Likens, G. E., C. T. Driscoll, D. C. Buso, T. G. Siccama, C. E. Johnson, G. M. Lovett, D. F. Ryan, T. Fahey, and W. A. Reiners (1994), The biogeochemistry of potassium at Hubbard Brook, *Biogeochemistry*, *25*(2), 61–125, doi:10.1007/BF00000881.

Monteith, D. T., et al. (2007), Dissolved organic carbon trends resulting from changes in atmospheric deposition chemistry, *Nature*, *450*(7169), 537–540, doi:10.1038/nature06316.

Nakićenović, N., R. Swart, J. Alcamo, and G. Davis (2000), *Special report on emissions scenarios: A special report of working group III of the Intergovernmental Panel on Climate Change*, 1st ed., Cambridge Univ. Press, Cambridge, U. K., 599 pp.

Norby, R. J., S. D. Wullschleger, C. A. Gunderson, D. W. Johnson, and R. Ceulemans (1999), Tree responses to rising CO_2 in field experiments: Implications for the future forest, *Plant Cell Environ.*, *22*(6), 683–714, doi:10.1046/j.1365-3040.1999.00391.x.

Norby, R. J., J. M. Warren, C. M. Iversen, B. E. Medlyn, and R. E. McMurtrie (2010), CO_2 enhancement of forest productivity constrained by limited nitrogen availability, *Proc. Natl. Acad. Sci. U. S. A.*, *107*(45), 19368–19373, doi:10.1073/pnas.1006463107.

Northeast Climate Impact Assessment (NECIA) (2006), Climate change in the U.S. northeast, a report of the northeast climate impacts assessment, Union of Concerned Scientists (UCS), UCS Publications, Cambridge, Mass., 52 pp.

Nowak, R. S., D. S. Ellsworth, and S. D. Smith (2004), Functional responses of plants to elevated atmospheric CO_2: Do photosynthetic and productivity data from FACE experiments support early predictions?, *New Phytologist*, *162*(2), 253–280, doi:10.1111/j.1469-8137.2004.01033.x.

Ollinger, S. V., J. D. Aber, and P. B. Reich (1997), Simulating ozone effects on forest productivity: Interactions among leaf-, canopy-, and stand-level processes, *Ecol. Appl.*, *7*(4), 1237–1251, doi:10.1890/1051-0761(1997)007[1237:SOEOFP]2.0.CO;2.

Ollinger, S. V., J. D. Aber, P. B. Reich, and R. J. Freuder (2002), Interactive effects of nitrogen deposition, tropospheric ozone, elevated CO_2 and land use history on the carbon dynamics of northern hardwood forests, *Global Change Biol.*, *8*(6), 545–562, doi:10.1046/j.1365-2486.2002.00482.x.

Ollinger, S. V., C. L. Goodale, K. Hayhoe, and J. P. Jenkins (2009), Potential effects of climate change and rising CO_2 on ecosystem processes in northeastern U.S. forests, *Mitigation and Adaptation Strategies for Global Change*, *14*(1), 101–106, doi:10.1007/s11027-008-9157-2.

Pope, V. D., M. L. Gallani, P. R. Rowntree, and R. A. Stratton (2000), The impact of new physical parametrizations in the Hadley Centre Climate Model: HadAM3, *Clim. Dyn.*, *16*(2), 123–146, doi:10.1007/s003820050009.

Saxe, H., D. S. Ellsworth, and J. Heath (1998), Tree and forest functioning in an enriched CO_2 atmosphere, *New Phytologist*, *139*(3), 395–436, doi:10.1046/j.1469-8137.1998.00221.x.

Schecher, W. D., and C. T. Driscoll (1995), ALCHEMI: A chemical equilibrium model to assess the acid-base chemistry and speciation of aluminum in dilute solutions, in *Chemical Equilibrium and Reaction Models*, edited by R. Loeppert, A. P. Schwab, and S. Goldberg, pp. 325–356, Soil Sci. Soc. America, Madison, Wis.

Venterea, R. T., P. M. Groffman, M. S. Castro, L. V. Verchot, I. J. Fernandez, and M. B. Adams (2004), Soil emissions of nitric oxide in two forest watersheds subjected to elevated n inputs, *For. Ecol. Manage.*, *196*(2–3), 335–349, doi:10.1016/j.foreco.2004.03.028.

Washington, W. M., et al. (2000), Parallel climate model (PCM) control and transient simulations, *Clim. Dyn.*, *16*(10), 755–774, doi:10.1007/s003820000079.

Worrall, F., T. Burt, and R. Shedden (2003), Long term records of riverine dissolved organic matter, *Biogeochemistry*, *64*(2), 165–178, doi:10.1023/A:1024924216148.

Zhai, J., C. T. Driscoll, T. J. Sullivan, and B. J. Cosby (2008), Regional application of the PnET-BGC model to assess historical acidification of Adirondack lakes, *Water Resour. Res.*, *44*(1), W01421, doi:10.1029/2006WR005532.